



Supplement of

Aircraft measurements of aerosol and trace gas chemistry in the eastern North Atlantic

Maria A. Zawadowicz et al.

Correspondence to: John E. Shilling (john.shilling@pnnl.gov)

The copyright of individual parts of the supplement might differ from the article licence.

20 AMS calibration for quantification of methanesulfonic acid (MSA)

There are several published methods of calibrating the AMS signal for the presence of MSA (Phinney et al., 2006, Huang et al., 2017, Ovadnevaite et al., 2011, Ge et al., 2012, Hodshire et al., 2019), but they all concentrate on the presence of a characteristic MSA marker, CH_3SO_2^+ . In addition, there are two additional minor characteristic markers, CH_2SO_2^+ and CH_4SO_3^+ (Ge et al., 2012, Huang et al., 2017). A well-known difficulty in laboratory MSA calibrations is neutralization of the acidic aerosol by the presence of trace amount of ammonia in laboratory air and on surfaces (Hodshire et al., 2019). To overcome this difficulty, we adapt the approach detailed in Hodshire, et al. (2019) and first calibrate the AMS using the neutralized form of MSA, $\text{NH}_4\text{CH}_3\text{SO}_3$. To prepare the calibration solution, MSA was neutralized with ammonium hydroxide. The final concentration of the calibration solution was 75 mM. The calibration solution was aerosolized with a Collison-type atomizer (TSI 3076, Shoreview, MN) and dried using a Nafion dryer (5 slpm counter-flow). The resulting aerosol was size-selected with a Differential Mobility Analyzer (DMA) (TSI, Shoreview, MN) to 250, 300 and 350 nm (Supplementary Figure S2). The calibration was performed using simultaneous measurements of CH_3SO_3^- ion concentration derived from Condensation Particle Counter (CPC) particle counts (TSI 3776, Shoreview, MN). In order to derive CH_3SO_3^- ion concentration, density of 1.3 g/cm^3 and shape factor of 1 was assumed. AMS PTOF data were used to correct for multiply charged particles. Resulting calibrations are shown in Supplementary Figure S2, along with a reference AMS mass spectrum of laboratory-generated neutralized MSA.

To quantify MSA, we use the combination of the three characteristic marker ions ($\text{CH}_2\text{SO}_2^+ + \text{CH}_3\text{SO}_2^+ + \text{CH}_4\text{SO}_3^+$). Using the standard AMS approach, (neutralized) MSA concentration is given by

$$40 \quad [\text{MSA}] = \frac{C}{CE} \frac{MW_{\text{NO}_3}}{RIE_{\text{MSA}} I_{\text{NO}_3}} \frac{I_{\text{CH}_2\text{SO}_2} + I_{\text{CH}_3\text{SO}_2} + I_{\text{CH}_4\text{SO}_3}}{f_{(\text{CH}_2\text{SO}_2 + \text{CH}_3\text{SO}_2 + \text{CH}_4\text{SO}_3)}},$$

Where C is a proportionality constant accounting for instrument duty cycle, flow rate and unit conversions. CE is the AMS collection efficiency, RIE_{MSA} is the ionization efficiency of (neutralized) MSA expressed proportionally to the ionization efficiency of nitrate (I_{NO_3}), which is obtained by standard AMS NH_4NO_3 calibration. I_x expresses the signal of marker ion x in ion counts and $f_{(\text{CH}_2\text{SO}_2 + \text{CH}_3\text{SO}_2 + \text{CH}_4\text{SO}_3)}$ is the ratio of signal of the sum of the marker ions to the total (neutralized) MSA signal. If ion signal is expressed in nitrate-equivalent concentration units, the equation simplifies to

$$[\text{MSA}] = \frac{1}{CE RIE_{\text{MSA}} f_{(\text{CH}_2\text{SO}_2 + \text{CH}_3\text{SO}_2 + \text{CH}_4\text{SO}_3)}} (I_{\text{CH}_2\text{SO}_2} + I_{\text{CH}_3\text{SO}_2} + I_{\text{CH}_4\text{SO}_3}) = \frac{CF}{CE} (I_{\text{CH}_2\text{SO}_2} + I_{\text{CH}_3\text{SO}_2} + I_{\text{CH}_4\text{SO}_3})$$

50 Where $CF = \frac{1}{RIE_{\text{MSA}} f_{(\text{CH}_2\text{SO}_2 + \text{CH}_3\text{SO}_2 + \text{CH}_4\text{SO}_3)}}$ is defined as the calibration factor and $\frac{CF}{CE}$ the slope in the laboratory calibration plot in Supplementary Figure S2, and has been determined to be 7.2 ± 0.9 .

Next, we determine parameters RI_{MSA} , $f_{(\text{CH}_2\text{SO}_2 + \text{CH}_3\text{SO}_2 + \text{CH}_4\text{SO}_3)}$ and $f_{\text{CH}_3\text{SO}_2}$ directly and summarize then in Supplementary Table S2. The ratios of marker signals to the total (neutralized) MSA signal are derived from average neutralized MSA mass spectra (Supplementary Figure S2A). RI_{MSA} can be estimated with the ammonium balance method: using the previously calibrated RI_{NH_4} (4.1), RI_{MSA} is adjusted to balance the ammonium with its counter-ion, CH_3SO_3^- . This assumes complete neutralization of MSA in the AMS. Supplementary Table S2 compares these calibration parameters to previous literature estimates, showing a large spread in values, which underscores the importance of calibrating each AMS independently.

Using the slope of the calibration plot in Figure S2B and independently derived estimates of RI_{MSA} and $f_{(\text{CH}_2\text{SO}_2 + \text{CH}_3\text{SO}_2 + \text{CH}_4\text{SO}_3)}$, we can constrain the CE for the neutralized MSA used in laboratory calibrations as 0.61 ± 0.07 . This is the largest source of uncertainty in translating the calibrations to ambient measurements of MSA, as ambient MSA is more acidic than the neutralized laboratory MSA, which implies that the ambient particles less viscous, which is expected to affect CE (Middlebrook et al., 2012). If the CE of acidic form of MSA is assumed to be 1, the calibration factor CF is 4.4 ± 0.5 , as shown in Figure S2C. This CE-corrected calibration factor is used to translate ACE-ENA AMS measurements to MSA concentrations.

Using the laboratory MSA calibrations, we also calculate the fraction of MSA signal assigned to organic and sulfate, 64% and 36%, respectively (Supplementary Table S2). Some MSA ions, such as the three characteristic markers used in the calibration are organosulfates, which are classified as organic by the default AMS routine.

70 **Supplementary Table S1:** Summary of ACE-ENA flights and vertical profiles.

RF #	Flight date	Takeoff (local time)	Landing (local time)	Number of spiral profiles	Altitude range (m)	Location of spiral profiles (lat, lon)
<i>summer</i>						
1	6/21/17	11:28	15:10	2	100 - 3000	39.23, -28.35
						39.24, -28.37
2	6/23/17	10:46	14:04	4	100 - 2500	39.11, -28.03
						39.79, -29.53
						39.11, -28.01
						39.18, -28.15
3	6/25/17	10:34	14:25	2	100 - 1850	39.11, -28.04
						39.75, -29.27
4	6/26/17	8:30	12:15	2	100 - 3300	39.16, -28.19
						39.26, -28.40
5	6/28/17	9:07	12:29	2	100 - 1900	39.27, -28.31
						39.31, -27.80
6	6/29/17	10:30	14:34	2	100 - 5000	40.09, -28.06
						40.11, -28.02
7	6/30/17	9:27	13:16	2	100 - 2000	39.30, -27.78
						39.30, -28.33
8	7/3/17	10:37	14:48	2	100 - 2000	39.11, -28.01
						39.10, -28.03
9	7/4/17	8:33	12:06	4	100 - 2600	39.32, -28.30
						38.97 -28.25
						39.31, -28.30
						38.94, -28.24
10	7/6/17	8:23	11:48	3	100 - 1900	39.35, -28.04
						39.37, -28.01
						39.37, -28.02
11	7/7/17	10:33	13:49	2	100 - 3300	37.76, -27.14
						37.51, -26.85
12	7/8/17	8:36	12:43	4	100 - 3300	40.02, -27.15
						39.60, -26.68
						39.46, -26.51

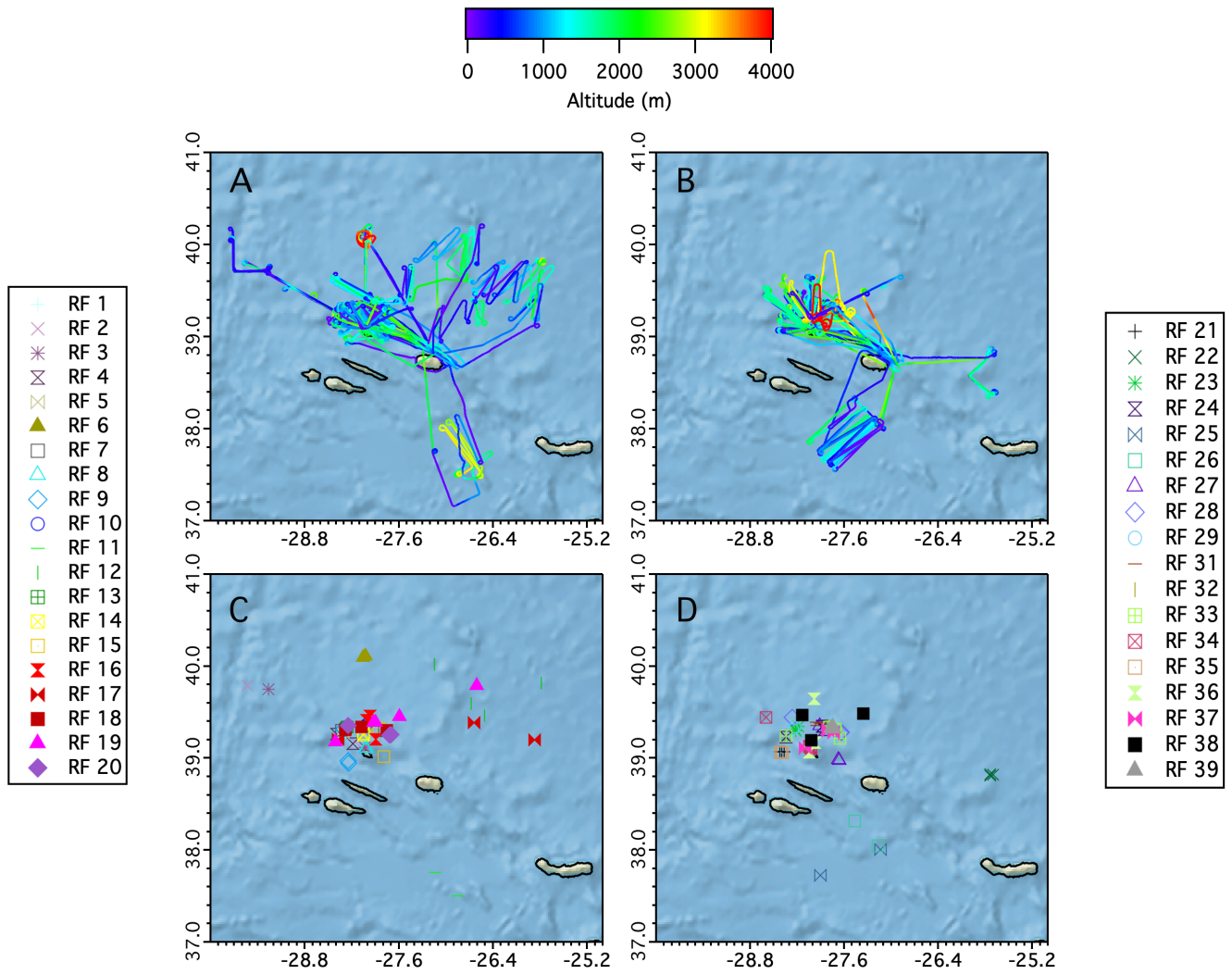
						39.82, -25.79
13	7/11/17	10:04	14:04	2	100 - 2500	39.32, -28.28
						39.34, -28.26
14	7/12/17	9:00	13:02	2	100 - 2100	39.25, -28.06
						39.27, -28.05
15	7/13/17	8:32	12:55	3	100 - 2000	39.33, -27.88
						39.33, -27.85
						39.02, -27.79
16	7/15/17	10:24	14:24	3	100 - 2000	39.21, -27.90
						39.46, -27.97
						39.41, -28.01
17	7/17/17	9:29	13:28	3	100 - 2000	39.21, -28.37
						39.39, -26.64
						39.20, -25.87
18	7/18/17	8:31	12:05	3	100 - 2500	39.34, -28.08
						39.30, -27.76
						39.31, -28.28
19	7/19/17	8:54	12:56	5	100 - 3000	39.17, -28.40
						39.39, -27.90
						39.38, -27.92
						39.45, -27.59
						39.79, -26.61
20	7/20/17	8:31	12:11	3	100 - 2500	39.25, -27.72
						39.26, -27.70
						39.35, -28.25
winter						
21	1/19/18	11:11	15:04	3	100 - 2000	39.07, -28.37
						39.07, -28.40
						39.07, -28.42
22	1/21/18	8:45	12:29	3	100 - 2600	38.81, -25.74
						38.82, -25.74
						38.82, -25.70
23	1/24/18	11:53	15:54	3	100 - 2600	39.31, -28.23
						39.30, -28.22
						39.34, -28.18

24	1/25/17	10:01	13:49	4	100 - 2600	39.31, -27.86
						39.23, -28.35
						39.35, -27.88
						39.35, -27.88
25	1/26/18	10:05	14:03	2	100 - 2000	38.01, -27.13
						37.73, -27.90
26	1/28/18	8:38	12:33	2	100 - 2700	38.05, -27.17
						38.32, -27.47
27	1/29/18	8:39	12:32	3	100 - 2600	38.97, -27.66
						38.98, -27.67
						39.35, -27.91
28	1/30/18	8:34	12:50	3	100 - 2600	39.28, -27.65
						39.44, -28.26
						39.28, -27.64
29	2/1/18	9:59	14:18	4	100 - 2700	39.28, -27.73
						39.31, -28.26
						39.34, -28.23
						39.37, -27.74
30	2/7/18	16:28	18:22	0	N/A	N/A
31	2/8/18	11:54	16:04	3	100 - 2300	39.39, -27.96
						39.38, -27.91
						39.36, -27.96
32	2/9/18	10:04	14:16	4	100 - 2500	39.36, -27.82
						39.25, -28.34
						39.35, -27.79
						39.32, -27.87
33	2/10/18	11:55	15:55	5	100 - 3800	39.34, -27.79
						39.31, -27.73
						39.31, -27.71
						39.24, -28.35
						39.22, -27.66
34	2/11/18	10:20	14:20	5	100 - 3900	39.13, -28.05
						39.10, -28.02
						39.11, -28.03
						39.44, -28.60

						39.12, -28.04
35	2/12/18	10:05	14:07	3	100 - 2500	39.07, -28.42
						39.06, -28.41
						39.06, -28.38
36	2/15/18	11:59	16:14	3	100 - 3700	39.17, -27.98
						39.64, -27.98
						39.06, -28.04
37	2/16/18	11:54	16:04	4	100 - 3700	39.31, -27.81
						39.28, -27.74
						39.11, -28.10
						39.30, -27.81
38	2/18/18	11:29	15:41	3	100 - 3200	39.48, -27.36
						39.19, -28.02
						39.47, -28.13
39	2/19/18	10:01	14:09	3	100 - 4000	39.32, -27.77
						39.31, -27.72
						39.35, -27.75

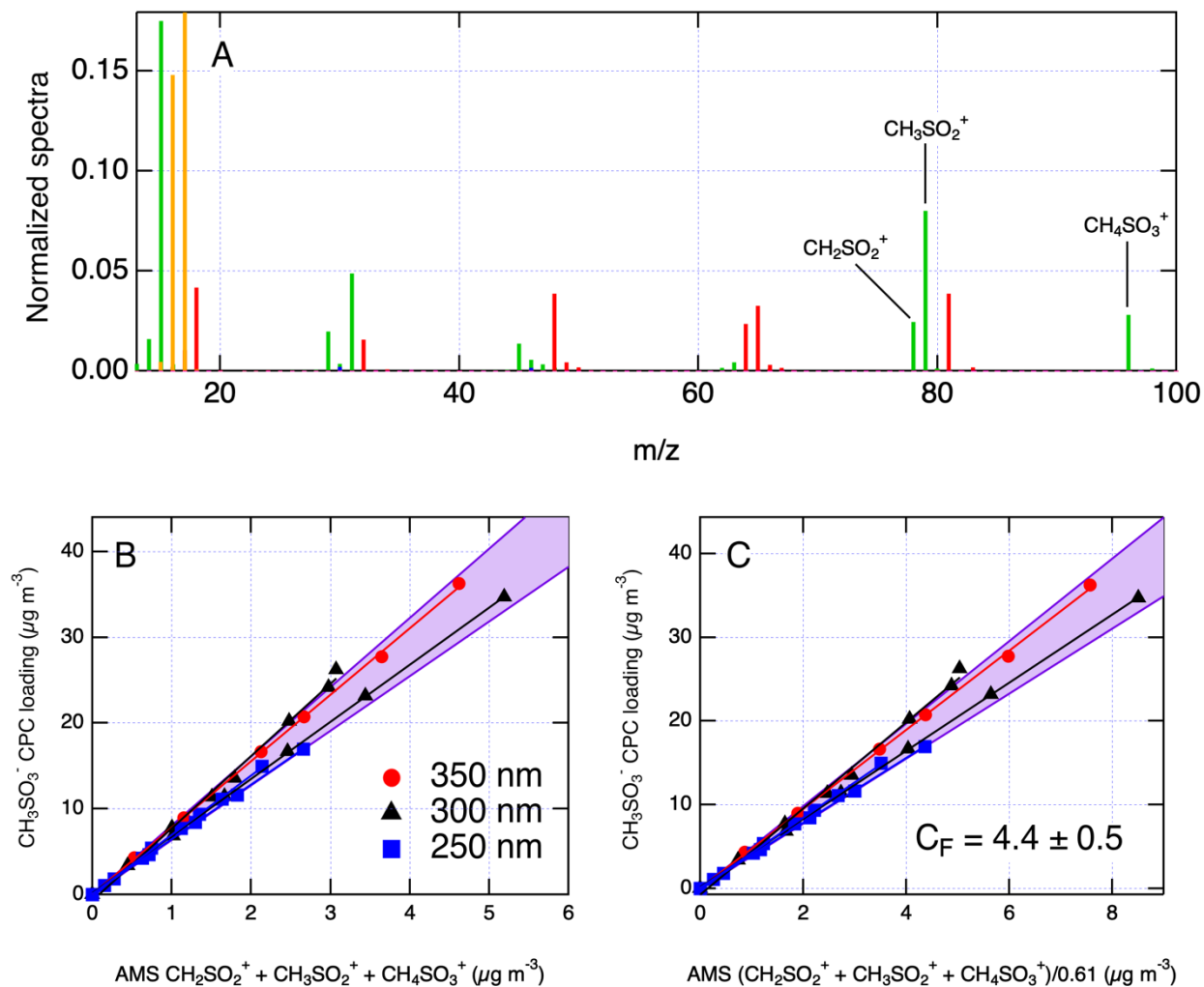
Supplementary Table S2: Calibration parameters for MSA in the PNNL AMS and comparisons to literature.

Parameter	This work	Previous estimates if available
MSA _{Org} (%)	63.9 ± 0.7	
MSA _{SO₄} (%)	36.1 ± 0.7	
RIE _{MSA} (UMR)	1.09 ± 0.02	1.33 (Willis et al., 2016), 1.27 (Huang et al., 2017),
RIE _{MSA} (HR)	0.87 ± 0.01	1.70 ± 0.08 (Hodshire et al., 2019)
f _{CH₃SO₂} (%)	15.9 ± 0.3	6.9 (Phinney et al., 2006), 9 (Zorn et al., 2008), 4 (Schmale et al., 2013), 9.7 (Huang et al., 2015), 12.4 (Willis et al., 2016), 4 (Huang et al., 2017), 7.9 (Hodshire et al., 2019)
f _(CH₂SO₂+CH₃SO₂+CH₄SO₃) (%)	26.1 ± 0.5	14.7 (Ge et al., 2012), 6.8 ± 0.6 (Huang et al., 2017)
Calibration factor (C _F)	4.4 ± 0.5	

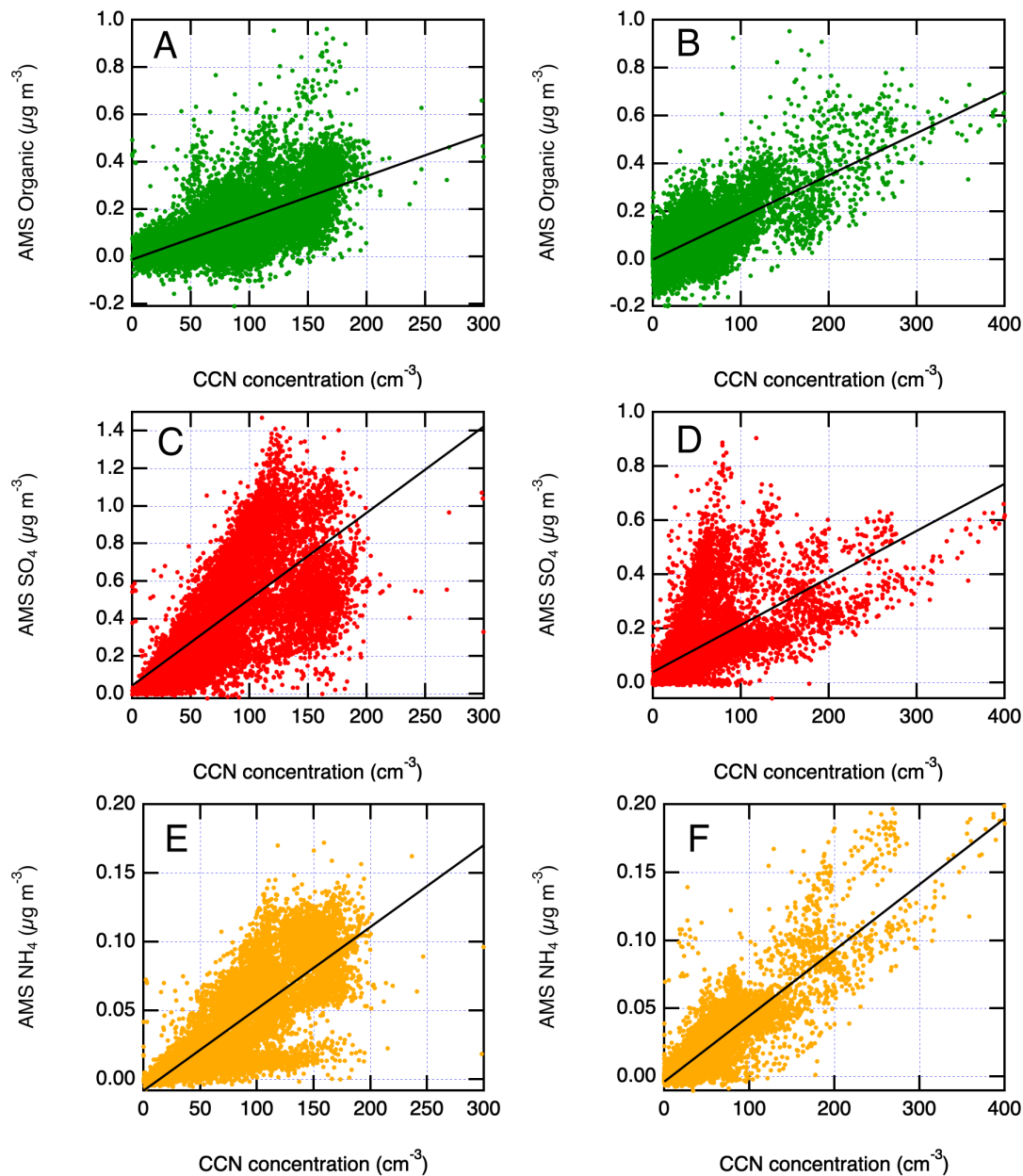


Supplementary Figure S1: Flight tracks for all G-1 flights carried out as a part of the ACE-ENA campaign. (A) All IOP 1 flight tracks. (B) All IOP 2 flight tracks. (C) Locations of spiral profiles for IOP 1. (D) Locations of spiral profiles for IOP 2.

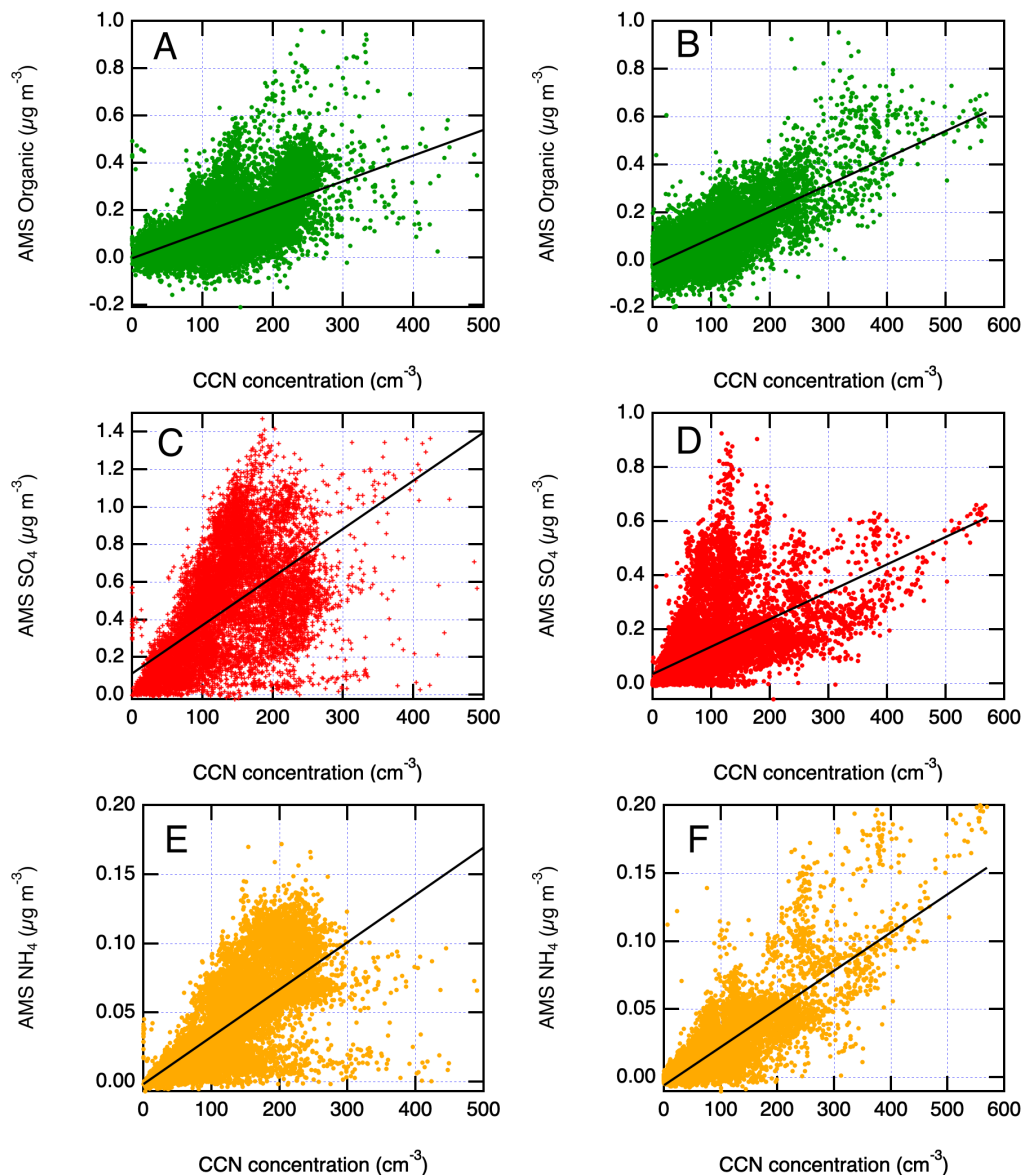
80 The map was created using public domain map data on Natural Earth (naturalearthdata.com) and the GSHHG Database (ngdc.noaa.gov/mgg/shorelines/).



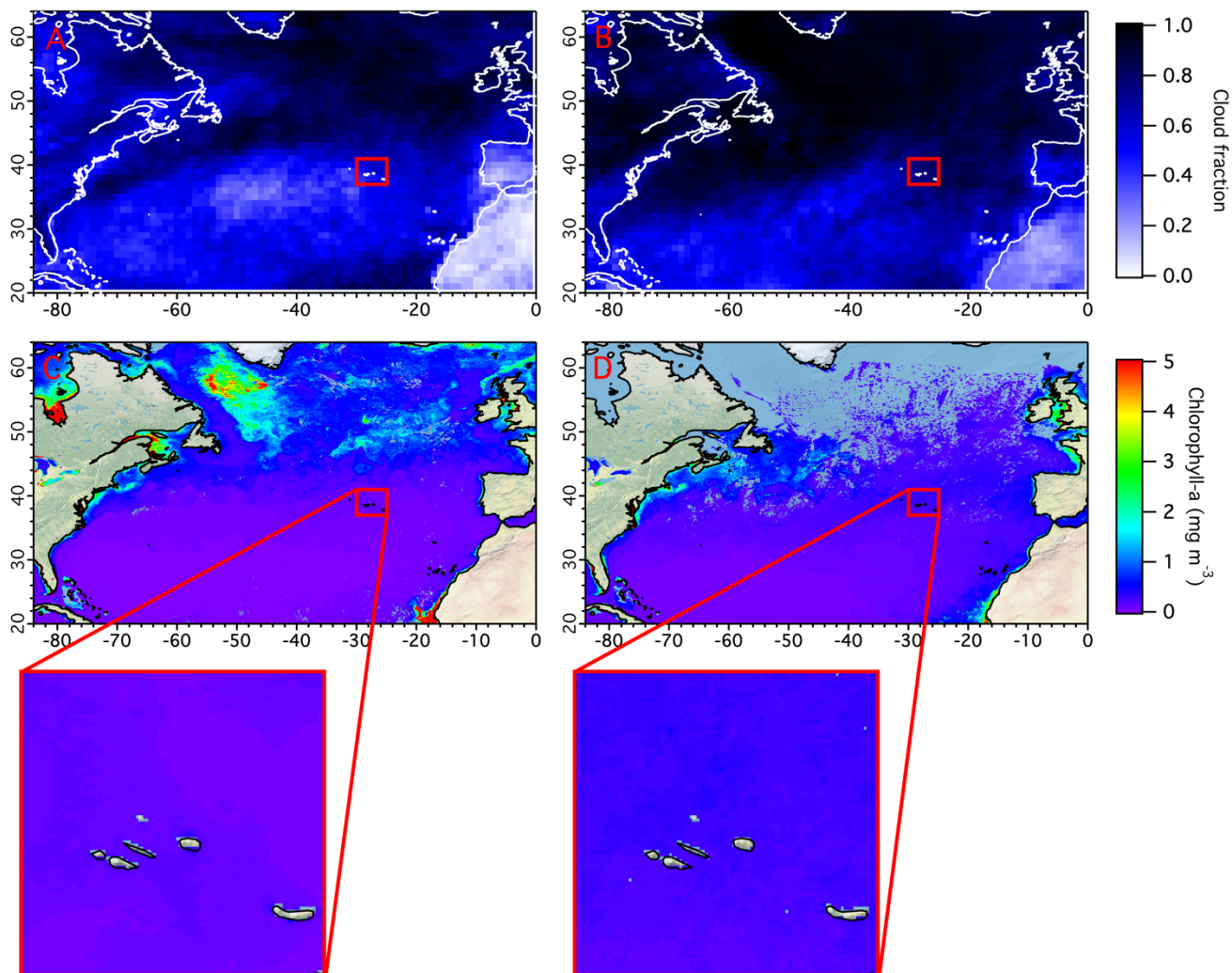
85 **Supplementary Figure S2:** Laboratory AMS calibrations for MSA. (A) Example spectrum of neutralized MSA used for the calibrations with key peaks labeled. (B) Calibrations using three different neutralized MSA sizes. Shaded region indicates uncertainty.



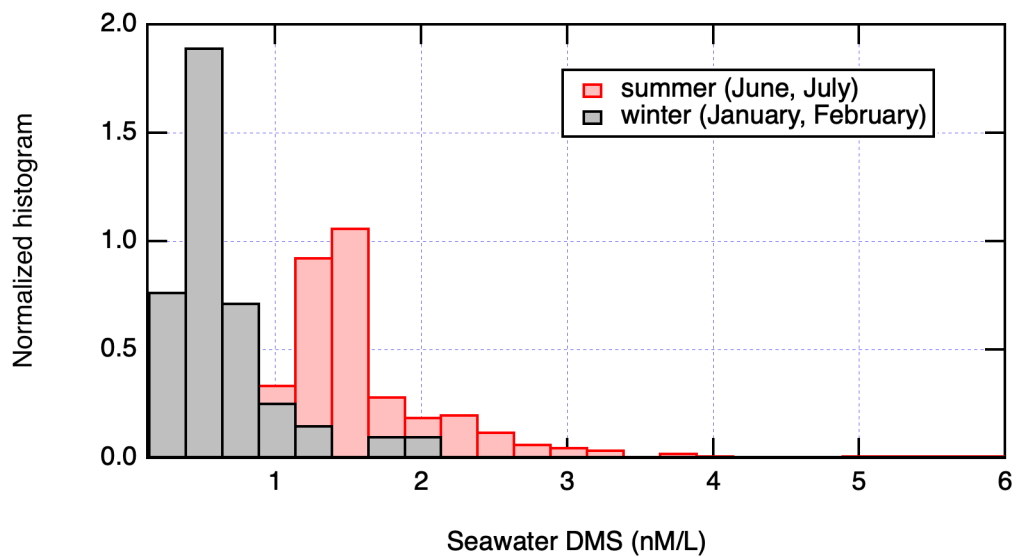
90 **Supplementary Figure S3:** Campaign-wide correlations between aerosol chemistry and CCN concentrations at 0.13% supersaturation. (A) AMS organic vs. CCN count, < 1000 m ($R^2 = 0.4$). (B) AMS organic vs. CCN count, > 1000 m ($R^2 = 0.5$). (C) AMS SO_4 vs. CCN count, < 1000 m ($R^2 = 0.5$). (D) AMS SO_4 vs. CCN count, > 1000 m ($R^2 = 0.4$). (E) AMS NH_4 vs. CCN count, < 1000 m ($R^2 = 0.6$). (F) AMS NH_4 vs. CCN count, > 1000 m ($R^2 = 0.8$).



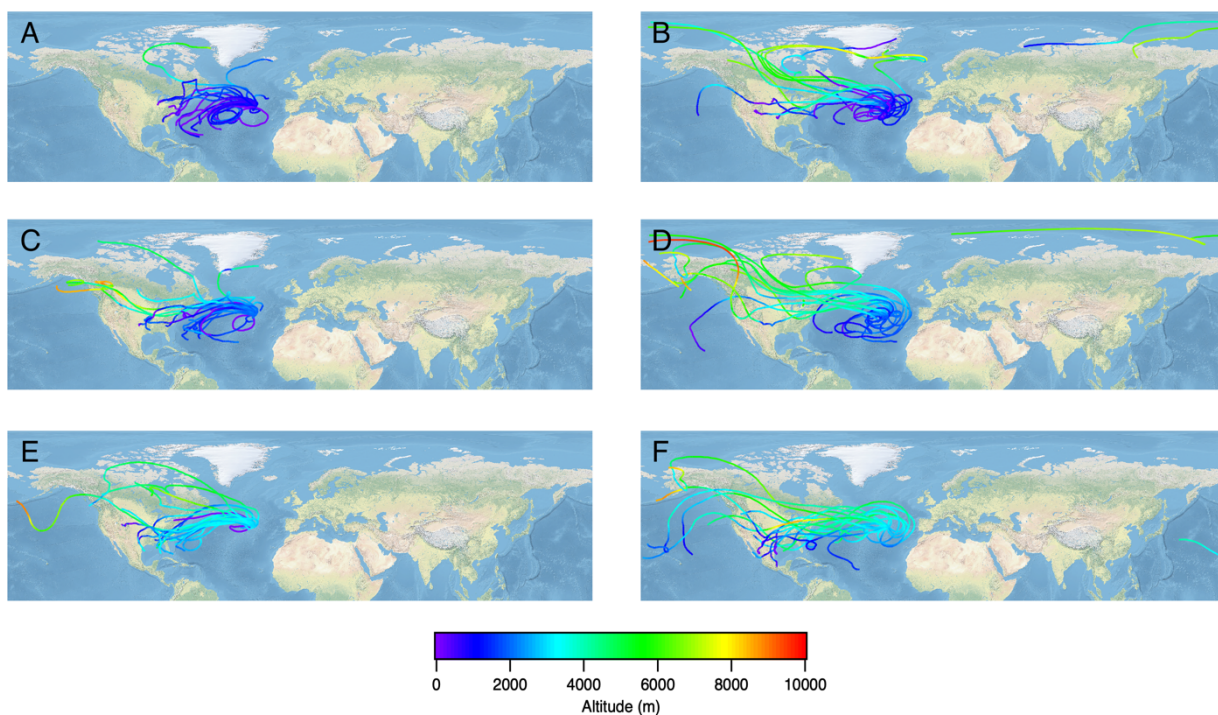
Supplementary Figure S4: Campaign-wide correlations between aerosol chemistry and CCN concentrations at 0.3% supersaturation. (A) AMS organic vs. CCN count, < 1000 m ($R^2 = 0.4$). (B) AMS organic vs. CCN count, > 1000 m ($R^2 = 0.6$). (C) AMS SO_4 vs. CCN count, < 1000 m ($R^2 = 0.4$). (D) AMS SO_4 vs. CCN count, > 1000 m ($R^2 = 0.3$). (E) AMS NH_4 vs. CCN count, < 1000 m ($R^2 = 0.5$). (F) AMS NH_4 vs. CCN count, > 1000 m ($R^2 = 0.7$).



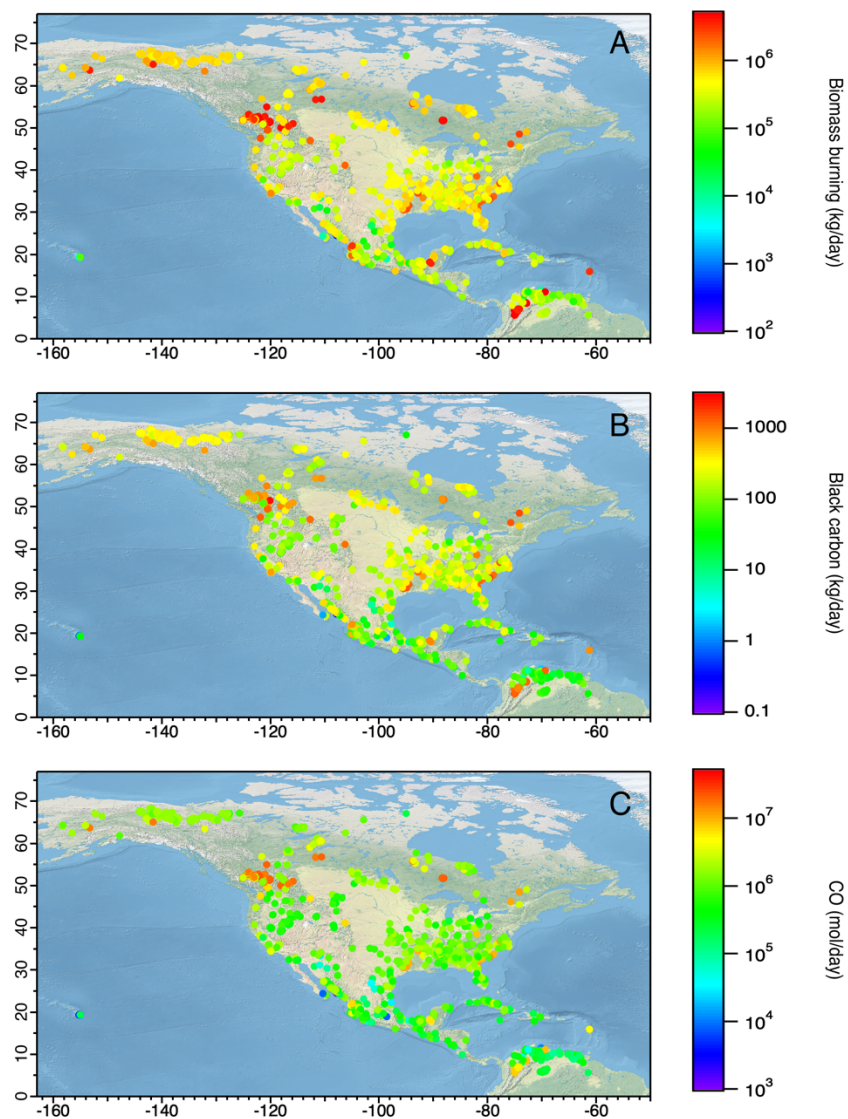
Supplementary Figure S5: Satellite measurements of relevant cloud and biogeochemical parameters during ACE-ENA. (A) MODIS Aqua time-averaged map of cloud fraction from cloud mask (count of lowest 2 clear sky confidence levels, cloudy and probably cloudy divided by the total count). Mean of daily mean, 1° resolution, from 06/21/2017 to 07/20/2017 (IOP 1) (Platnick, 2015). (B) Same as (A) but from 01/19/2018 to 02/19/2018 (IOP 2). (C) MODIS Aqua time-averaged map of chlorophyll-a concentration. Mean of 8-day means, 4 km resolution, 06/18/2017 to 07/28/2017 (IOP 1) (NASA Goddard Space Flight Center, 2018). (D) Same as (C) but from 01/17/2018 to 02/26/2018 (IOP 2). Red box indicates the Azores. The map was created using public domain map data on Natural Earth (naturalearthdata.com) and the GSHHG Database (ngdc.noaa.gov/mgg/shorelines/).



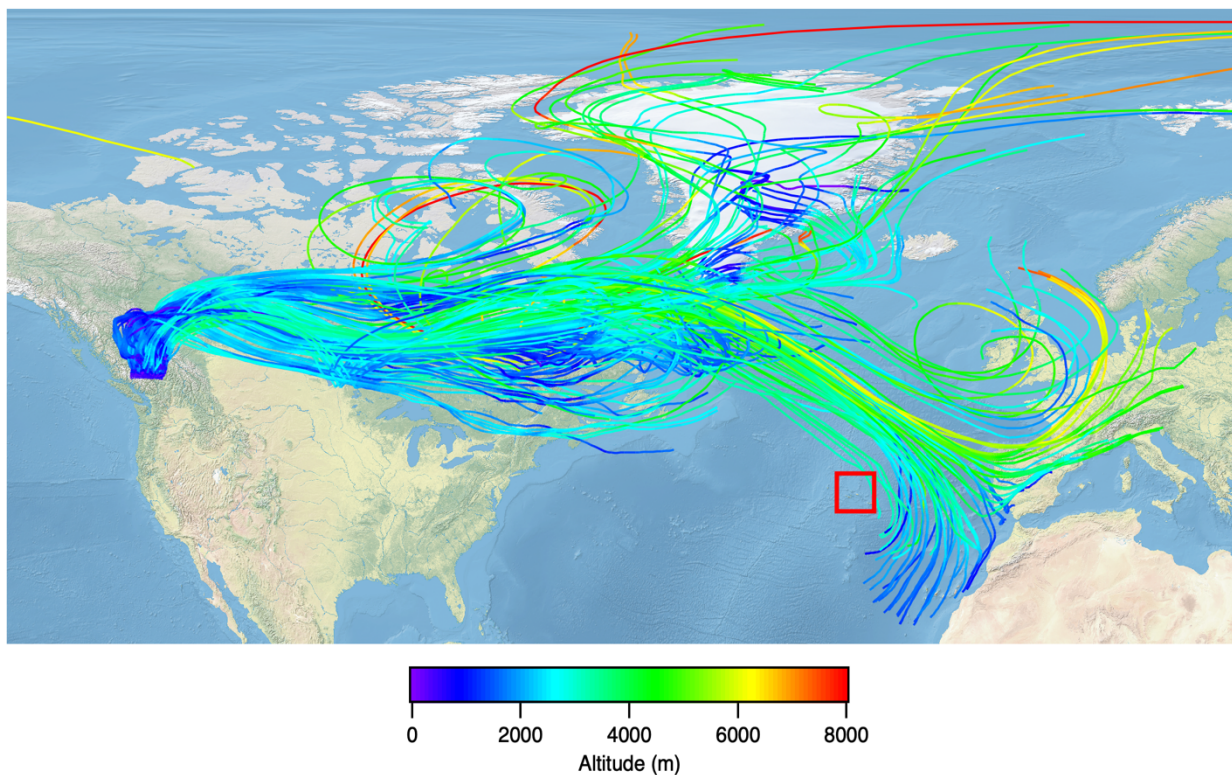
Supplementary Figure S6: The Global Surface Seawater DMS Database (saga.pmel.noaa.gov/dms/) (Kettle et al., 1999) was used to find surface seawater DMS measurements during January and February ($n = 78$) and June and July ($n = 293$) in latitudes between 30.7°N and 48.4°N and longitudes between 12.6°W and 38.4°W (enclosing the Azores).



Supplementary Figure S7: HYSPLIT 14-day back-trajectories for each flight. The starting point is the ENA ARM site. (A) 1000 m starting altitude, IOP 1. (B) 1000 m starting altitude, IOP 2. (C) 2000 m starting altitude, IOP 1. (D) 2000 m starting altitude, IOP 2. (E) 3000 m starting altitude, IOP 1. (F) 3000 m starting altitude, IOP 2. The map was created using public domain map data on Natural Earth (naturalearthdata.com) and the GSHHG Database (ngdc.noaa.gov/mgg/shorelines/).



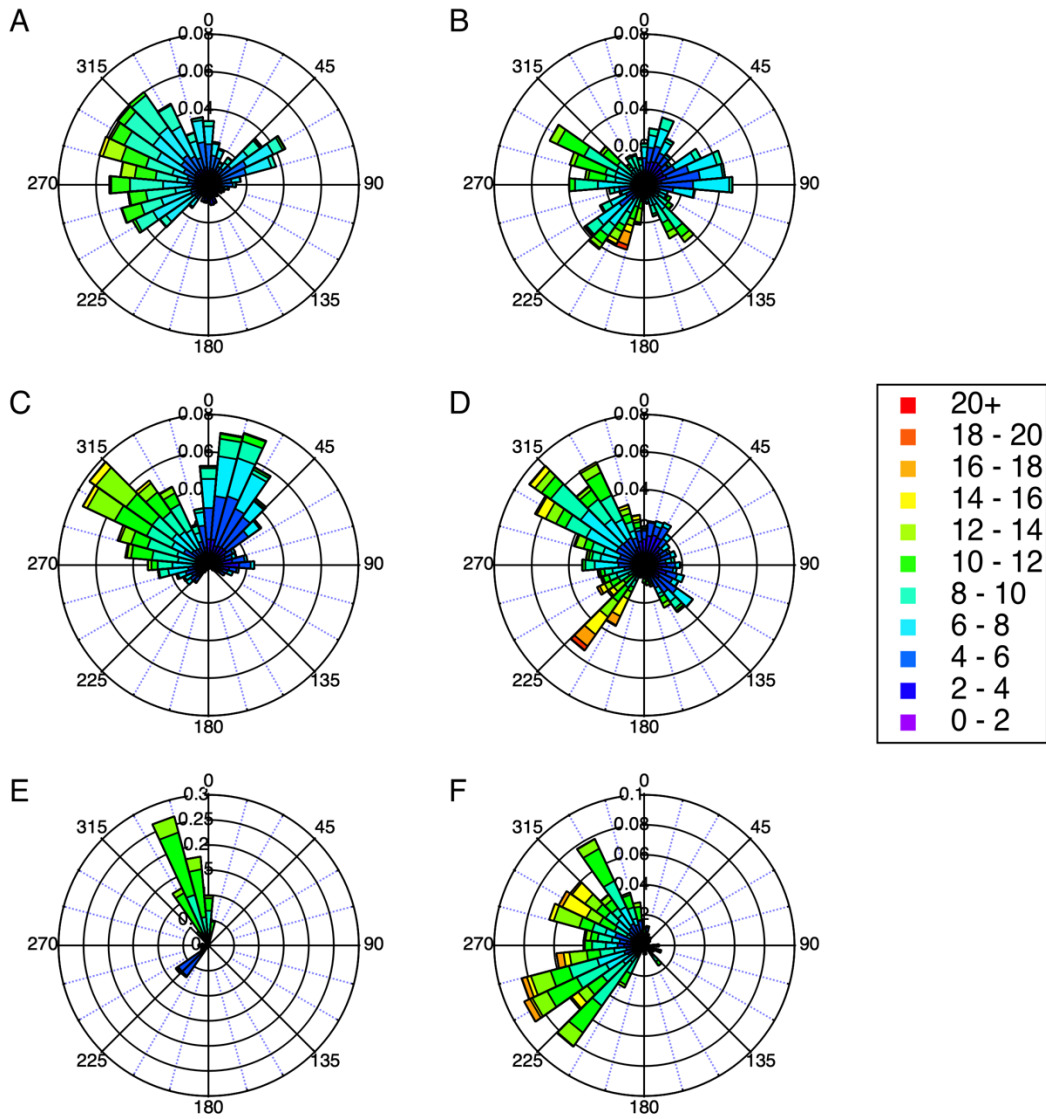
125 **Supplementary Figure S8:** Fire emissions during July 12 - 15, 2017 estimated using the Fire Inventory from NCAR (FINN) (Wiedinmyer et al., 2011). (A) Biomass burning emissions. (B) Black carbon emissions. (C) CO emissions. The map was created using public domain map data on Natural Earth (naturalearthdata.com) and the GSHHG Database (ngdc.noaa.gov/mgg/shorelines/).



130

Supplementary Figure S9: HYSPLIT trajectory analysis for the case study of RF #19 (July 19, 2017). A matrix of 121 10-day forward-trajectories was started from an evenly spaced grid bounded by (53.4 N, 125 W), (53.4 N, 121 W), (51 N, 125 W) and (51 N, 121 W) at 500 m altitude. GDAS 0.5 degree meteorology and isentropic vertical motion were used. The red box indicates the location of the Azores. The map was created using public domain map data on Natural Earth (naturalearthdata.com) and the GSHHG Database (ngdc.noaa.gov/mgg/shorelines/).

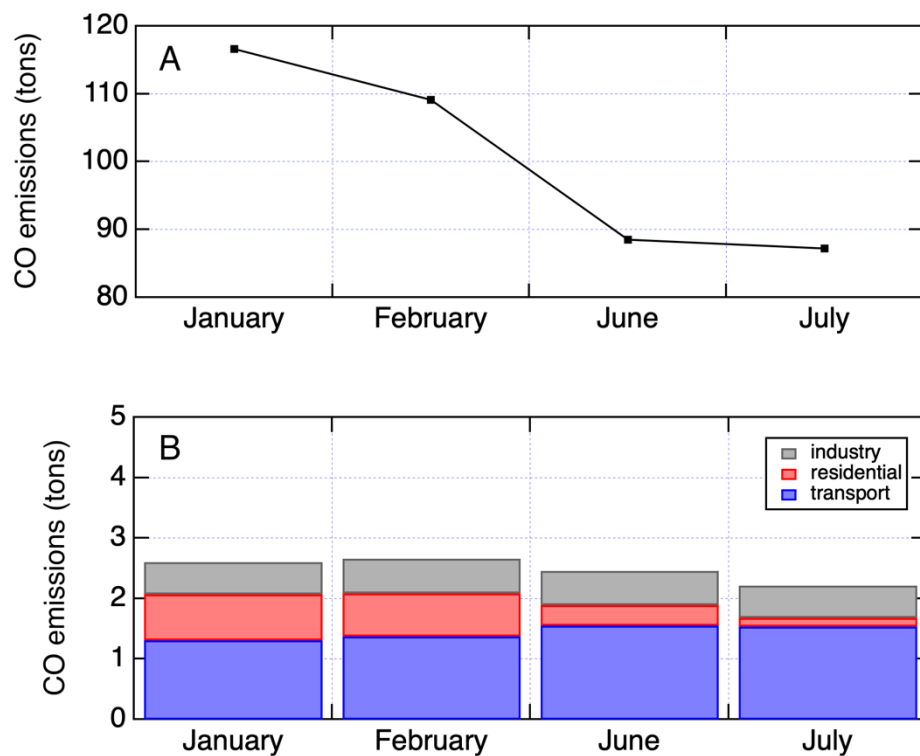
135



Supplementary Figure S10: Wind roses plotted using data from the G-1 AIMMS-20 probe during all ACE-ENA flights.

(A) < 1000 m altitude, IOP 1. (B) < 1000 m altitude, IOP 2. (C) 1000 m - 3000 m altitude, IOP 1. (D) 1000 m - 3000 m

140 altitude, IOP 2. (E) > 3000 m altitude, IOP 1. (F) > 3000 m altitude, IOP 2.



Supplementary Figure S11: EDGAR-HTAP V2 (https://edgar.jrc.ec.europa.eu/htap_v2/) gridded emissions inventory (Janssens-Maenhout et al., 2015) was used to investigate CO emissions from the Azores during the four months of ACE-
145 ENA study. Monthly gridmaps 0.1x0.1 for 2010 were used for this plot. (A) CO emissions from the energy sector. Data from one gridpoint at 38.7°N, 27.2°W is available for the Azores. (B) CO emissions from industry, residential and transport sectors. Data from 87 gridpoints are available for the Azores (34°N - 42°N, 20°W - 35°W), averages by sector are reported in the plot.

- Ge, X., Zhang, Q., Sun, Y., Ruehl, C. R., and Setyan, A.: Effect of aqueous-phase processing on aerosol chemistry and size distributions in Fresno, California, during wintertime, *Environmental Chemistry*, 9, 10.1071/en11168, 2012.
- Hodshire, A. L., Campuzano-Jost, P., Kodros, J. K., Croft, B., Nault, B. A., Schroder, J. C., Jimenez, J. L., and Pierce, J. R.: The potential role of methanesulfonic acid (MSA) in aerosol formation and growth and the associated radiative forcings, *Atmospheric Chemistry and Physics*, 19, 3137-3160, 10.5194/acp-19-3137-2019, 2019.
- 155 Huang, D. D., Li, Y. J., Lee, B. P., and Chan, C. K.: Analysis of organic sulfur compounds in atmospheric aerosols at the HKUST supersite in Hong Kong using HR-ToF-AMS, *Environ Sci Technol*, 49, 3672-3679, 10.1021/es5056269, 2015.
- Huang, S., Poulain, L., van Pinxteren, D., van Pinxteren, M., Wu, Z., Herrmann, H., and Wiedensohler, A.: Latitudinal and Seasonal Distribution of Particulate MSA over the Atlantic using a Validated Quantification Method with HR-ToF-AMS, *Environ Sci Technol*, 51, 418-426, 10.1021/acs.est.6b03186, 2017.
- 160 Janssens-Maenhout, G., Crippa, M., Guizzardi, D., Dentener, F., Muntean, M., Pouliot, G., Keating, T., Zhang, Q., Kurokawa, J., Wankmüller, R., Denier van der Gon, H., Kuenen, J. J. P., Klimont, Z., Frost, G., Darras, S., Koffi, B., and Li, M.: HTAP_v2.2: a mosaic of regional and global emission grid maps for 2008 and 2010 to study hemispheric transport of air pollution, *Atmospheric Chemistry and Physics*, 15, 11411-11432, 10.5194/acp-15-11411-2015, 2015.
- 165 Kettle, A. J., Andreae, M. O., Amouroux, D., Andreae, T. W., Bates, T. S., Berresheim, H., Bingemer, H., Boniforti, R., Curran, M. A. J., DiTullio, G. R., Helas, G., Jones, G. B., Keller, M. D., Kiene, R. P., Leck, C., Levasseur, M., Malin, G., Maspero, M., Matrai, P., McTaggart, A. R., Mihalopoulos, N., Nguyen, B. C., Novo, A., Putaud, J. P., Rapsomanikis, S., Roberts, G., Schebeske, G., Sharma, S., Simó, R., Staubes, R., Turner, S., and Uher, G.: A global database of sea surface dimethylsulfide (DMS) measurements and a procedure to predict sea surface DMS as a function of latitude, longitude, and month, *Global Biogeochemical Cycles*, 13, 399-444, 10.1029/1999gb900004, 1999.
- 170 Middlebrook, A. M., Bahreini, R., Jimenez, J. L., and Canagaratna, M. R.: Evaluation of Composition-Dependent Collection Efficiencies for the Aerodyne Aerosol Mass Spectrometer using Field Data, *Aerosol Science and Technology*, 46, 258-271, 10.1080/02786826.2011.620041, 2012.
- NASA Goddard Space Flight Center, O. E. L., Ocean Biology Processing Group.: Moderate-resolution Imaging Spectroradiometer (MODIS) Aqua Chlorophyll Data; 2018 Reprocessing, in, NASA OB.DAAC, Greenbelt, MD, USA, 2018.
- 175 Ovadnevaite, J., O'Dowd, C., Dall'Osto, M., Ceburnis, D., Worsnop, D. R., and Berresheim, H.: Detecting high contributions of primary organic matter to marine aerosol: A case study, *Geophysical Research Letters*, 38, n/a-n/a, 10.1029/2010gl046083, 2011.
- 180 Phinney, L., Richard Leaitch, W., Lohmann, U., Boudries, H., Worsnop, D. R., Jayne, J. T., Toom-Saunty, D., Wadleigh, M., Sharma, S., and Shantz, N.: Characterization of the aerosol over the sub-arctic north east Pacific Ocean, *Deep Sea Research Part II: Topical Studies in Oceanography*, 53, 2410-2433, 10.1016/j.dsr2.2006.05.044, 2006.
- Platnick, S.: MODIS Atmosphere L3 Daily Product, in, edited by: System, N. M. A. P., Goddard Space Flight Center, USA, 2015.
- 185 Schmale, J., Schneider, J., Nemitz, E., Tang, Y. S., Dragosits, U., Blackall, T. D., Trathan, P. N., Phillips, G. J., Sutton, M., and Braban, C. F.: Sub-Antarctic marine aerosol: dominant contributions from biogenic sources, *Atmospheric Chemistry and Physics*, 13, 8669-8694, 10.5194/acp-13-8669-2013, 2013.
- Wiedinmyer, C., Akagi, S. K., Yokelson, R. J., Emmons, L. K., Al-Saadi, J. A., Orlando, J. J., and Soja, A. J.: The Fire INventory from NCAR (FINN): a high resolution global model to estimate the emissions from open burning, *Geoscientific Model Development*, 4, 625-641, 10.5194/gmd-4-625-2011, 2011.
- 190 Willis, M. D., Burkart, J., Thomas, J. L., Köllner, F., Schneider, J., Bozem, H., Hoor, P. M., Aliabadi, A. A., Schulz, H., Herber, A. B., Leaitch, W. R., and Abbatt, J. P. D.: Growth of nucleation mode particles in the summertime Arctic: a case study, *Atmospheric Chemistry and Physics*, 16, 7663-7679, 10.5194/acp-16-7663-2016, 2016.
- Zorn, S. R., Drewnick, F., Schott, M., Hoffmann, T., and Borrmann, S.: Characterization of the South Atlantic marine boundary layer aerosol using an aerodyne aerosol mass spectrometer, *Atmospheric Chemistry and Physics*, 8, 4711-4728, 10.5194/acp-8-4711-2008, 2008.